Polymer 50 (2009) 1671–1681

Contents lists available at ScienceDirect

Polymer

journal homepage: www.elsevier.com/locate/polymer

Degradation of a sulfonated aryl ether ketone model compound in oxidative media (sPAEK)

Carine Perrot [a], Laurent Gonon [a,*], Michel Bardet [a,c], Catherine Marestin [b], Alain Pierre-Bayle [a,c], Gérard Gebel [a]

[a] Institut Nanosciences et Cryogénie, Laboratoire ≪Structure et Propriétés d'Architectures Moléculaires≫ SPrAM, UMR 5819 CEA-CNRS-UJF, Equipe "Polymères Conducteurs Ioniques", 17 rue des Martyrs, 38054 Grenoble cedex 9, France
[b] Laboratoire des Matériaux Organiques à Propriétés Spécifiques, UMR 5041, CNRS, Chemin du Canal, 69360, Solaize, France
[c] Institut Nanosciences et Cryogénie, SCIG, Laboratoire de Résonances Magnétiques, 17 rue des Martyrs, 38054 Grenoble, France

ARTICLE INFO

Article history:
Received 27 June 2008
Received in revised form
22 December 2008
Accepted 23 December 2008
Available online 22 January 2009

Keywords:
sPAEK
Polymer degradation
Fuel cell

ABSTRACT

Poor durability of polymer electrolyte membranes is one of the most limiting factors of proton exchange membrane fuel cell (PEMFC). Hydrogen peroxide which is formed electrochemically or chemically during operation is one of the potential deteriorating factors, particularly for polyaromatic membranes. To be able to increase membrane durability, the aging path involved must be elucidated. To give an insight into the degradation mechanism of sulfonated polyaryl ether ketones (sPAEK) a study on model compound has been performed. Each species produced has been collected by liquid chromatography and identified by NMR, IR and mass spectroscopies. We have demonstrated that degradation proceeds through the addition of a hydroxyl radical on the aromatic ring. Then, the oxidation of these phenolic groups leads to several chain scissions. On the basis of these experiments, a strategy can be drawn to improve the membrane durability.

1. Introduction

Nafion®, a perfluorosulfonic acid polymer commercialized by DuPont de Nemours, is the most widely used proton conductive membrane to prepare Membrane Electrode Assembly (MEA) for fuel cell applications. It fulfils almost all physical characteristics required, such as high proton conductivity, good thermal stability, suitable mechanical strength and excellent chemical stability. However, its high price and the environmental risks related to its disposal have motivated the research of non-perfluorinated, aromatic-heterocyclic membranes which could be more environmentally friendly [1]. On the basis of the different structures envisioned among alternative polymer electrolytes, sulfonated polybenzimidazoles (sPBI [2–6]), sulfonated polyimides (sPI [7–16]), sulfonated polyaryl ether sulfones (SPAES [17–20]) and sulfonated polyaryl ether ketones (sPAEK [21–27]) have been the most extensively studied. A particular interest emerged in recent years about sPAEK synthesized by direct polycondensation of sulfonated monomers [21,28]. These materials are considered as particularly promising owing to the excellent thermal stability, low sensitivity to oxidation and to hydrolysis of their unsulfonated homologous.

Whereas the performances of membranes made from such polymers are in some cases comparable to those obtained with Nafion, to date, none of these materials meet the required specifications, especially concerning the lifetime.

While mechanical aging processes such as successive swelling–deswelling cycles can induce some membrane fragility, chemical degradations are suspected to be the major factors limiting the durability of these alternative polymers [1,29–40]. As H_2O_2 has already been detected in the water produced during a fuel cell test performed with Nafion membrane [36], hydroxyl radicals ($HO^{\bullet}$) are suspected to be responsible for oxidative degradation reactions. Although hydrocarbon PEMs are shown to be susceptible to oxidative degradation in the H_2O_2 ex-situ test environment, nevertheless, they have been shown to have lifetimes of several thousand hours in fuel cells [16,20]. Detailed mechanistic studies have already been reported concerning the degradation of Nafion in the presence of hydroxyl radicals [41–44]. However, only qualitative tests have been performed up to now on alternative membranes. For example, chemical aging in Fenton's reagent is currently used as an accelerated test to simulate fuel cell

* Corresponding author. Tel.: +33 4 38 78 93 33; fax: +33 4 38 78 56 91.
E-mail address: Laurent.gonon@cea.fr (L. Gonon).

0032-3861/$ – see front matter © 2009 Elsevier Ltd. All rights reserved.
doi:10.1016/j.polymer.2008.12.051

conditions, and the membrane stability is estimated from the time required to become brittle. However, a wide range of experimental conditions are reported for such tests (H_2O_2 concentrations ranging from 3% [21,45] to 30% [28,46], test temperatures varying from 30 °C to 100 °C, as well as ferrous salt concentration which can go from 2 ppm to 30 ppm [21,28,45,46]). As a consequence, results described in the literature are difficult to compare and do not allow a good understanding of the degradation processes. It is important to outline that ex-situ aging in hydroperoxide solution only provides an insight as to possible degradation routes in particular for high concentrations of H_2O_2 relative to what would be found in the fuel cell operating conditions. Indeed, a too high radical concentration could induce additional routes of degradation limiting the membrane life time.

In order to get a better insight into the degradation mechanism, a thorough isolation and characterization of the species produced during an aging process appear fundamental. Such an approach is unfortunately very difficult to achieve on polymers themselves. Indeed, because of the structural complexity of starting materials that leads to a mixture of different species like oligomers after aging, identification of the chemical changes induced on the backbone becomes very difficult to achieve. In particular, end chain modifications are of interest because they are characteristic of chain scissions and have a significant impact on the physical properties of the material.

Therefore, the strategy adopted in this study relies on the identification of the species that are produced during the aging process (in the presence of H_2O_2) of a model compound. This compound was designed to be representative of the chemical structure of a sulfonated poly(aryl ether ketone). This methodology has already been applied with success by Geniès et al. [8] to study the hydrolytical stability of polyimide and by Maréchal et al. [47] to study the thermal and electrochemical stability of ionomers. In order to study the evolution of the aging medium, chemical structures of the main degradation products were determined through successive oxidation steps. Based on the results obtained, a degradation mechanism was proposed.

2. Experimental section

2.1. Materials

Phenol, N-methylpyrrolidinone (NMP) and potassium carbonate (K_2CO_3), were used as received. 4,4′-Difluoro-3,3′-disodium sulfonate benzophenone was prepared according to the procedure described by Wang [48]. A 30% hydrogen peroxide solution was used to prepare aging solution.

2.2. Model compound synthesis (M)

In a three-necked round bottom flask equipped with a mechanical stirrer and a nitrogen inlet, 7.7 g (1.82×10^{-2} mol) of 4,4′-difluoro-3,3′-disodium sulfonate benzophenone, 3.68 g (3.92×10^{-2} mol) of phenol and 6.04 g (4.3×10^{-2} mol) of potassium carbonate were suspended in 24 g of NMP. The reaction mixture was heated at 200 °C for 24 h. After cooling, the medium was precipitated into an ethanol/acid mixture. The precipitated white powder was filtered out, washed with ether and dried at 80 °C under vacuum. IR valence vibrations (KBr, cm^{-1}): 1658 (C═O); 1602, 1588, 1493, 1478 (C═C); 1205, 1251 (Ar–O–Ar); 1235, 1196, 1086, 1033 (O═S═O). ^1H NMR (400 MHz, D_2O, 1 wt%): δ(ppm) 8.32 (d, 2.3 Hz, 2H, H_{B5}); 7.84 (dd, 8.8 Hz, 2.3 Hz, 2H, H_{B3}); 7.51 (t, 7.9 Hz, 4H, H_{A2}); 7.33 (t, 7.9 Hz, 2H, H_{A1}); 7.23 (d, 7.9 Hz, 4H, H_{A3}); 6.99 (d, 8.8 Hz, 2H, H_{B2}). ^{13}C NMR (400 MHz, D_2O, 1 wt%): δ(ppm) 194.56 (1C, C═O); 159.04 (2C, C_{B1}); 154.64 (2C, C_{A4}); 134.98 (2C, C_{B3}); 132.78 (2C, $C_{B4\ or\ B6}$); 131.14 (2C, C_{B5}); 130.62 (4C, C_{A2}); 130.25 (2C, $C_{B4\ or\ B6}$); 125.78 (2C, C_{A1}); 120.70 (4C, C_{A3}); 117.07 (2C, C_{B2}). MS (negative mode): m/z 525 $[M-H]^-$; 262 $[M-2H]^{-2}/2$.

2.3. Aging conditions

Different mixtures containing various proportions of Model (M) and H_2O_2 were prepared using stock solutions of both compounds. Samples will be labelled as follows: $(RX/[H_2O_2]/\theta)$, where $X = n_{H_2O_2}/n_M$ corresponds to the molar ratio R of hydrogen peroxide versus model compound M, $[H_2O_2]$ is the concentration of hydrogen peroxide and θ the aging temperature.

Pure water was used to prepare these solutions in order to avoid any catalytic hydrogen peroxide decompositions with metallic residues. Degradation experiments were performed in sealed glass tubes, with R ranging from 0.25 to 4, $[H_2O_2]$ from 0.045 to 0.7 vol% and temperatures from 60 to 130 °C. Aging bath volume was adjusted according to the target of the experiment. For example, typical volume was 2 cm^3 for kinetic experiments by NMR whereas a volume of about 50 cm^3 was used to prepare samples for chromatographic analyses.

This range of hydroperoxide concentration is based on previous work performed on sulfonated polyimide membrane [11]. For this range of concentration, it has been checked that no additional routes of degradation were induced due to a too important instantaneous radical concentration.

After the aging treatments, samples were freeze-dried before characterization.

2.4. Measurements

2.4.1. Chromatographic separation

HPLC analyses were carried out using an Agilent 1100 Series (autosampler G1313A, quaternary pump G1311A, UV detector G1315B, fraction collector G1364C). Analytical and preparative separations were performed using specific columns. The mobile phase was composed of a mixture of water with 5 mM ammonium acetate (solvent A) and acetonitrile (solvent B). Ammonium salt was used as a buffer to minimize random variations of the retention times which are due to the ionic nature of the analysed products. The added salt permits also to refine chromatographic peaks. To optimize the separation, a gradient method was performed. Data were processed using the Agilent Chemstation software (version B.01.01).

2.4.1.1. Analytical chromatographic separation (LC–MS). The analytical HPLC method used was able to separate model molecules from all aged products of interest. The experimental conditions were the following: column, a reverse phase 300 SB-C18 (4.6×250 mm, 5 μm); mobile phase flow rate, 1 ml/min; linear solvent gradient, 0–30 min 99–75% (solvent A); injection volume, 3 μl of a 5 mg/ml solution. Phase separation was monitored by UV absorption at 295 and 254 nm and mass spectrum detection. These two wavelengths were found to be characteristic of all the products. Mass spectra were acquired using a LC/MSD SL (G 1956B) mass spectrometer equipped with an electrospray source used to ionize the molecules. The solutions were analysed in the negative mode, scanning from 200 to 600 mass units every 1 s. Additional analyses on collected fractions have been performed by direct infusion through fused silica tubing at 2–10 μl min^{-1}.

2.4.1.2. Preparative chromatographic separation (HPLC). To perform additional structural identification of each fractioned species, preparative phase separation was achieved using a semi-preparative Zorbax SB-C18 column (9.4×50 mm, 5 μm). Experimental

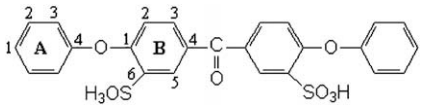

Fig. 1. Chemical structure of model compound (M).

conditions applied were: mobile phase flow rate, 2 ml/min; solvent gradient, 0–9 min 99–80% (solvent A), 9–10 min 80–80% (solvent A); injection volume, 20 μl of a 5 mg/ml solution. A gradual return to the initial conditions was performed before the next injection. As only one wavelength can be selected to collect the eluted fraction, the effluent was monitored at 210 nm, an absorption wavelength shared by all degradation products.

Each collected species was freeze-dried before their structural identification by ^{1}H, ^{13}C NMR, IR and mass spectroscopy.

2.4.2. Spectroscopic analyses

2.4.2.1. Infrared (IR). Infrared spectra were recorded on a Nicolet Magna System 750 FTIR spectrometer and data were processed using OMNIC software. Analyses were performed in transmission mode on KBr pellets with a nominal resolution of 2 cm^{-1} and 32 scans summation.

2.4.2.2. Nuclear magnetic resonance (NMR). High-resolution liquid NMR was carried out with a Varian Unity 400 MHz NMR spectrometer operating at a resonance frequency of 399.960 MHz for ^{1}H and 100.58 MHz for ^{13}C. Spectra were recorded at 25 °C using a 5 mm inverse detection probe. Some assignments were made with 2D NMR using an inverse-probe with field gradients for correlation spectroscopy (COSY), heteronuclear multiple quantum correlation (HMQC) and heteronuclear multiple bond correlation (HMBC). Products were dissolved in deuterated water (D_2O) and the chemical shift of 2,2,3,3-d(4)-3-(trimethylsilyl)-propionic acid sodium salt (TsP-d_4) was used as the internal standard reference.

3. Results and discussion

Model compound (M) (Fig. 1), representative of the hydrophilic sequences of a sulfonated poly(arylether ketone) obtained by direct polycondensation, was synthesized by aromatic nucleophilic substitution, according to known procedures.

3.1. Preliminary observations

^{1}H NMR spectrum of a model compound (M) sample treated for 1500 h at 130 °C in D_2O (sealed tube) is identical to those of the starting compound (Fig. 2). These observations confirm the well-known stability of aryl ether ketone structures in water and suggest that whereas desulfonation has already been reported for aromatic sulfonated groups [49–51], such a phenomenon is not significant after 1500 h at 130 °C.

An interesting ^{1}H NMR feature of the model compound (M) has to be outlined. ^{1}H NMR spectra of different solutions with increasing model compound concentrations are reported in Fig. 3. We observe a significant decrease in the chemical shift values when the model compound concentration increases. A variation as high as 0.3 ppm is measured when the solution concentration raises from 1 to 5 wt%. This variation is most striking for protons present on the sulfonated aromatic ring (B2 and B3).

This unexpected phenomenon can easily be explained by intermolecular interactions that increase as the concentration is raised. The associations probably occurred between sulfonic and ketonic groups of two different molecules. Sulfonic groups are ionic, hence dissociated in water. This explanation is strengthened by the effect of NEt_4^+, Br^- addition (5 wt%). This salt is known to screen ionic interactions and therefore it induces the same effect as a concentration decreases (Fig. 3). To confirm this hypothesis, D_2O was replaced by DMSO in order to reduce sulfonic group dissociation. As expected, no effect of the model molecule concentration on chemical shift values could be evidenced in this case. The identification of degradation products by NMR analysis of the mixture is not an easy task. Moreover, the overlap of some characteristic bands does not allow a complete quantification. Therefore, it is appealing to begin the analysis by a separation process.

3.2. Qualitative analysis

3.2.1. Model compound degradation

Three identical samples ($R2/[0.58]/\theta$) were respectively heated at 60, 80 and 130 °C. In all cases, aging time was adjusted to ensure complete hydrogen peroxide decomposition. The samples were first freeze-dried and then solubilized in deuterated solvent before proton NMR analysis. As expected, the amount of degradation products is all the more important that the aging temperature is high (Fig. 4). This shows that radicals are more effective at higher temperature or produced in a bigger amount since each solution initially contains the same concentration of H_2O_2 and model compound (M).

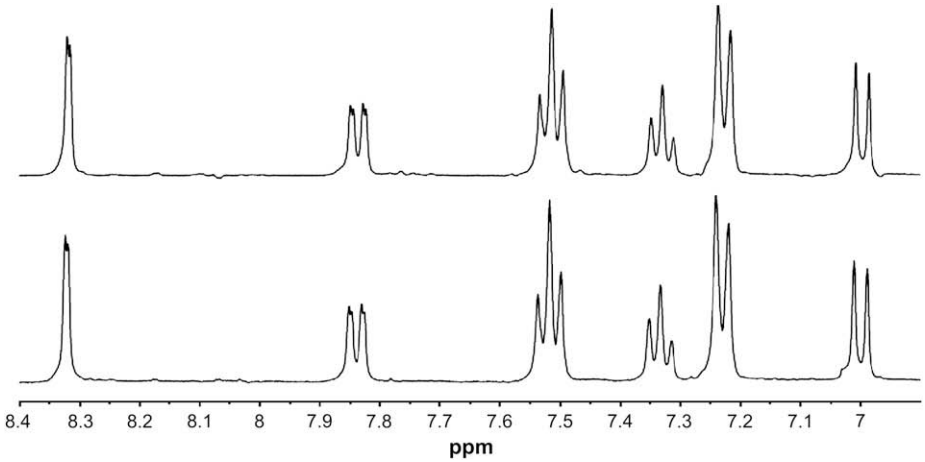

Fig. 2. ^{1}H NMR spectra of model compound (M) in D_2O (1 wt%): a) virgin; b) aged at 130 °C for 1500 h.

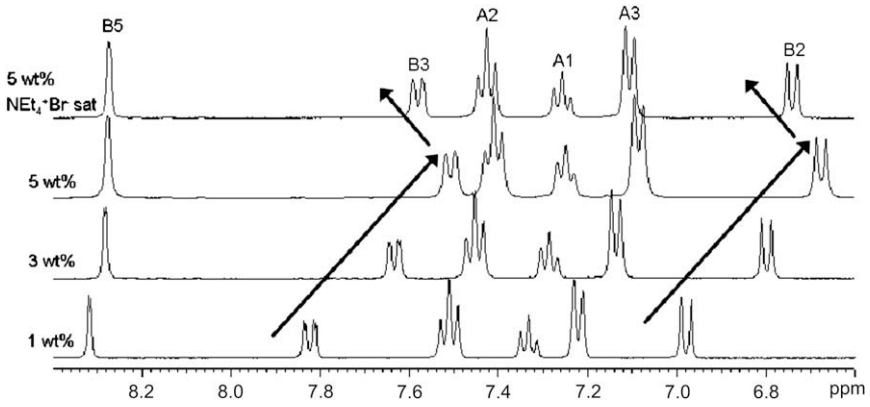

Fig. 3. ^{1}H NMR spectra of model compound (M) in D_2O at different concentrations.

However, the nature of the degradation products does not seem to be influenced by the treatment temperature. As mentioned above, the slight chemical shift deviations can be attributed to concentration variations.

3.2.2. Identification of the degradation products

A high performance liquid chromatographic analysis was performed on a sample aged at 130 °C (*R*2/[0.58]/130 °C) for 24 h in order to evidence the most significant degradation products. Typical chromatograms recorded at a wavenumber of 254 and 295 nm are reported in Fig. 5. Apart from the remaining model compound (M) (elution time 25.8 min), seven main other products (A, B, C, D, E, E′, E″) are present. The UV absorption and mass spectra of each species were recorded. If no significant information on their molecular structure can be deduced from this analysis, it is worth noticing that three eluted products E* (E, E′, E″ respectively eluted at 21.9, 23.6 and 26.3 min) have the same UV absorption spectra with a main maximum at 295 nm as well as the same *m*/*z* value at 541. This suggests the presence of three isomers.

In order to unambiguously identify the chemical structure of the degradation products, preparative chromatography analyses were performed to collect large amounts of each fraction to proceed to IR, NMR and MS analyses. To illustrate the methodology applied, extensive analyses performed on the collected fraction associated with the elution peak at 18.5 min (product D) are shown in Fig. 6.

The mass spectrum shown in Fig. 6-1 indicates that the molecular weight of this product is 450 g/mol. Indeed we can notice the presence of [M−H] ion at *m*/*z* 449, as well as adduct ions associated to sodium and potassium respectively at *m*/*z* 471 and *m*/*z* 487, and the presence of [M−2H]/2 ion at *m*/*z* 224. IR spectrum (Fig. 6-2) allowed to identify the valence vibration characteristic of the main chemical functions. Thus, the analysed product possesses an aromatic structure (C=C, 1600, 1585, 1480 and 1490 cm^{-1}) and carbonyl (C=O, 1652 cm^{-1}), alcohol (O–H, 3500–3100 cm^{-1}), ether (–O–, 1245 and 1193 cm^{-1}) and sulfonic groups (–SO_3H, 1086 and 1028 cm^{-1}). Finally, ^{1}H and ^{13}C NMR analyses (Fig. 6-3 and -4) allowed to determine the chemical structure of this product which is presented in Table 1. Whereas the proportion of the protons present on the non-substituted aromatic ring (noted A1, A2 and A3) are reduced from half of their initial value recorded on the ^{1}H NMR spectra of M, the three additional peaks observed (noted C2, C3 and C6) are characteristic of a 1,3,4-tri-substituted aromatic ring. Chemical shifts of this spectrum are consistent with a structure in which an ether bridge has been replaced by a phenol group. ^{13}C NMR spectrum (Fig. 6-2) confirms the above mentioned structure. Expected chemical shifts for compound D have been calculated using the semi-empirical technique [52,53] and the calculated values are consistent with the expected data.

According to the same strategy, all degradation products collected by preparative HPLC were identified. They are gathered in Table 1. Except for the addition products E* (E, E′ and E″), the

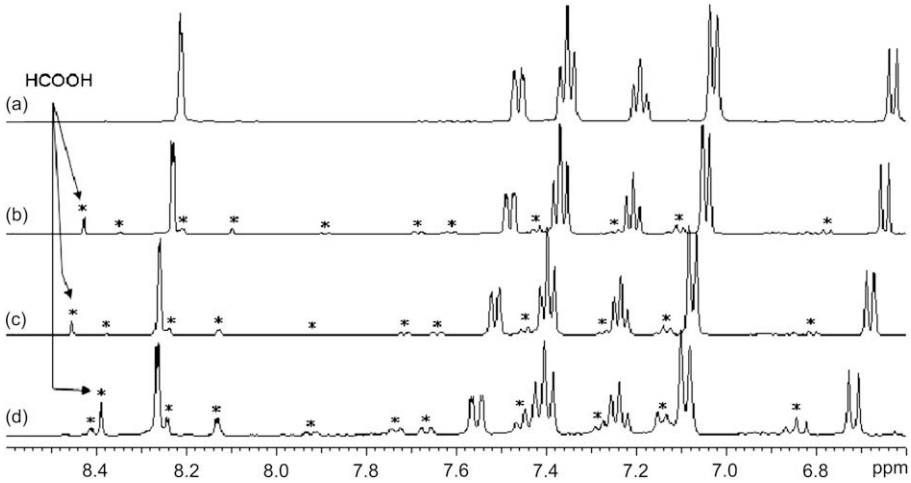

Fig. 4. ^{1}H NMR spectra in D_2O (room temp) of model compound aged in H_2O_2 (*R*2/[0.58]/θ): a) unaged model compound; b) aged compound $\theta = 60$ °C/620 h; c) aged compound $\theta = 80$ °C/85 h; d) aged compound $\theta = 130$ °C/24 h. *Degradation products.

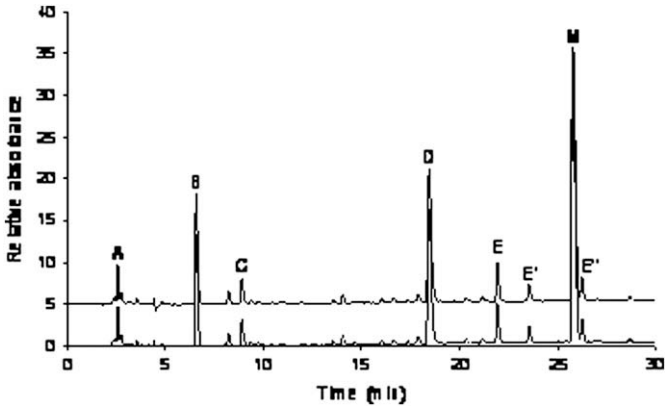

Fig. 5. LC–MS chromatograms of model compound aged *R*2/0.58/130 °C ($\lambda = 254$ and 295 nm).

identified degradation products are induced by a scission around ether and ketone linkages.

Product A. IR valence vibrations: not detected, the fraction is mainly composed of ammonium acetate salt. ^{1}H NMR (400 MHz, D_2O, 1 wt%): δ(ppm) 7.07 (d, 8.1 Hz, 1H, H_2); 7.93 (d, 8.1 Hz, 1H, H_3); 8.21 (s, 1H, H_5). ^{13}C NMR (400 MHz, D_2O, 1 wt%): δ(ppm) 156 (1C, C_1); 134.5 (1C, C_3); 129.3 (1C, C_5). MS (negative mode): *m*/*z* 217 $[M-H]^-$. **Product B**. IR valence vibrations (KBr, cm^{-1}): 3500–3100 (O–H); 1697 (C═O); 1589, 1479, 1493 (C═C); 1255, 1200 (–O–); 1183, 1240, 1085, 1029 ($-SO_3H$). ^{1}H NMR (400 MHz, D_2O, 1 wt%): δ(ppm) 7.27 (t, 7.3 Hz, 1H, H_{A1}); 7.46 (t, 7.7 Hz, 2H, H_{A2}); 7.16 (d, 8.1 Hz, 2H, H_{A3}); 6.93 (d, 8.8 Hz, 1H, H_{B2}); 7.91 (dd, 8.8 Hz, 2 Hz, 1H, H_{B3}); 8.34 (d, 2 HZ, 1H, H_{B5}). ^{13}C NMR (400 MHz, D_2O, 1 wt%): δ(ppm) 125 (1C, C_{A1}); 130.4 (2C, C_{A2}); 120.2 (2C, C_{A3}); 155.7 (1C, C_{A4}); 157.1 (1C, C_{B1}); 118.2 (1C, C_{B2}); 134 (1C, C_{B3}); 131.9 and 129.5 (1C, $C_{B4 \text{ and } B6}$); 129.6 (1C, C_{B5}); 173.9 (1C, $C_{C=O}$). MS (negative mode): *m*/*z* 293 $[M-H]^-$; 146 $[M-2H]^{-2}$. **Product C**. IR valence vibrations: Insufficient amount to be analysed. ^{1}H NMR (400 MHz, D_2O, 1 wt%): δ(ppm) 7.05 (d, 8.8 Hz, 2H, H_2); 7.82 (dd, 8.8 Hz–1.6 Hz, 2H, H_3); 8.13 (d, 1.6 Hz, 2H, H_5). ^{13}C NMR (400 MHz, D_2O, 1 wt%): δ(ppm) 161.2 (2C, C_1); 135.6 (2C, C_3); 128.3 (2C, C_4); 131.2 (2C, C_5); 126.7 (2C, C_6); 196.7 (1C, $C_{C=O}$). MS (negative mode): *m*/*z* 373 $[M-H]^-$; 186 $[M-2H]^{-2}$. **Product D**. IR valence vibrations: 3500–3100 (O–H); 1652 (C═O); 1600, 1585, 1480, 1490 (C═C); 1245, 1193 (–O–); 1086, 1028 ($-SO_3H$). ^{1}H NMR (400 MHz, D_2O, 1 wt%): δ(ppm) 7.31 (t, 7.5 Hz, 1H, H_{A1}); 7.5 (t, 8.0 Hz, 2H, H_{A2}); 7.21 (d, 8.0 Hz, 2H, H_{A3}); 6.99 (d, 8.6 Hz, 1H, H_{B2}); 7.81 (dd, 8.6–2.2 Hz, 1H, H_{B3}); 8.27 (d, 2.2 Hz, 1H, H_{B5}); 7.85 (dd, 8.6 Hz–2.2 Hz, 1H, H_{C2}); 7.1 (d, 8.6 Hz, 1H, H_{C3}); 8.16 (d, 2.2 Hz, 1H, H_{C6}). ^{13}C NMR (400 MHz, D_2O, 1 wt%): δ(ppm) 125.5 (1C, C_{A1}); 130.4 (2C, C_{A2}); 120.5 (2C, C_{A3}); 155 (1C, C_{A4}); 158.7 (1C, C_{B1}); 117.6 (1C, C_{B2}); 135 (1C, C_{B3}); 132 and 131.5 (1C, $C_{B4 \text{ and } B6}$); 130.7 (1C, C_{B5}); 128.6 and 127.1 (1C, $C_{C1 \text{ and } C5}$); 136 (1C, C_{C2}); 117.5 (1C, C_{C3}); 160.8 (1C, C_{C4}); 131 (1C, C_{C6}); 196.5 (1C, $C_{C=O}$). MS (negative mode): *m*/*z* 449 $[M-H]^-$; 224 $[M-2H]^{-2}$. **Product E′** (–OH in *meta* position). IR valence vibrations: Insufficient amount to be analysed. ^{1}H NMR (400 MHz, D_2O, 1 wt%): δ(ppm) 7.35 (t, 8.3 Hz, 1H, H_{A1}); 7.53 (t, 8.3 Hz, 2H, H_{A2}); 7.26 (d, 8.3 Hz, 2H, H_{A3}); 6.88 and 6.92 (d, 8.1 Hz, 1H, $H_{B2 \text{ and } C3}$); 7.89 (m, 2H, $H_{B3 \text{ and } C2}$);

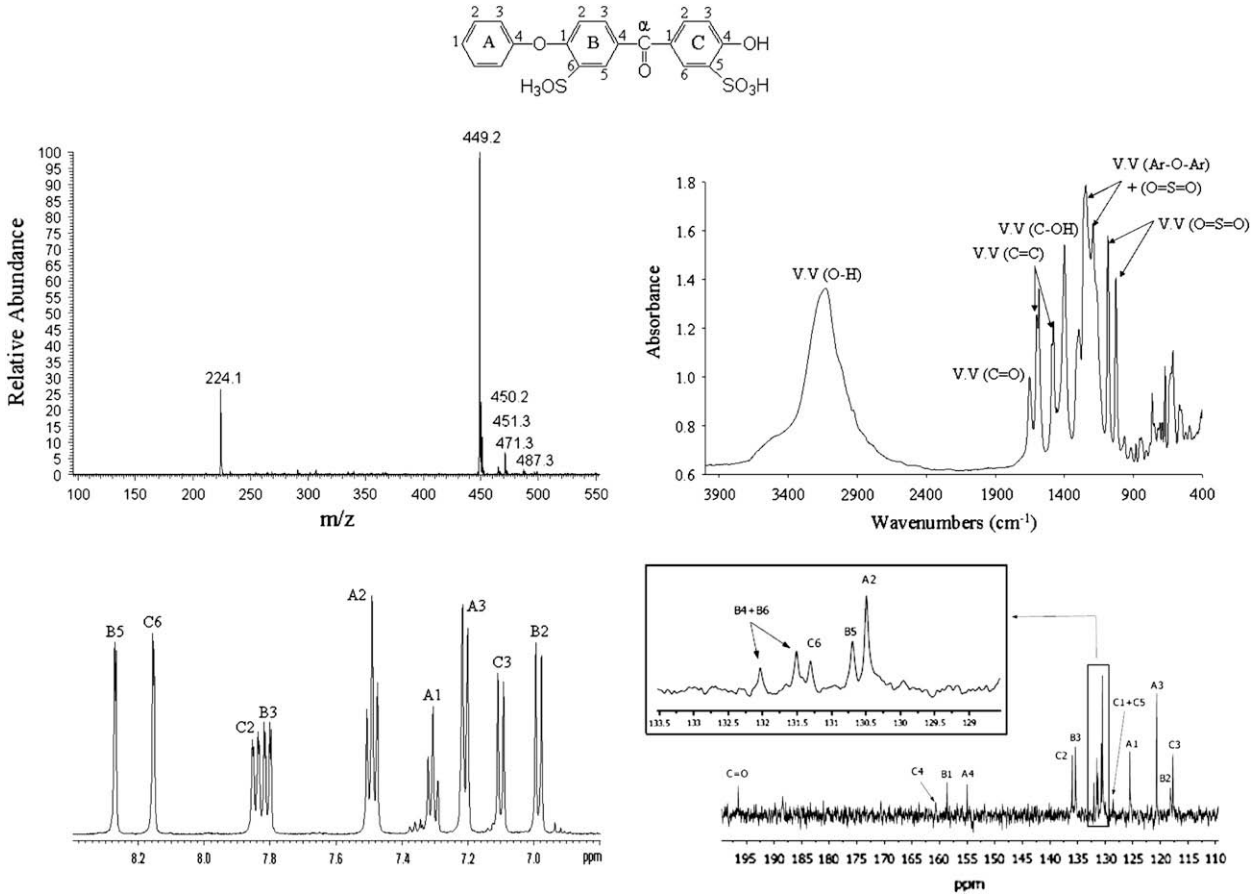

Fig. 6. Elucidation of D chemical structure: 1) MS spectrum, 2) IR spectrum, 3) ^{1}H NMR spectrum; 4) ^{13}C NMR spectrum.

Table 1
Degradation products nature of the model compound aging in *R*2/0.58/130 °C, their MS, IR and NMR characteristics.

	RT[a] (min)	Product chemical structure
A	2.6	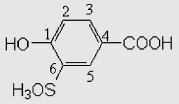
B	6.6	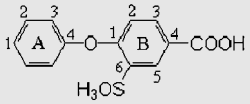
C	8.9	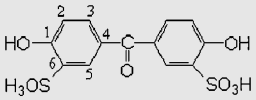
D	18.5	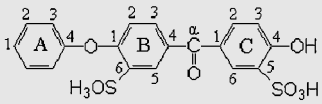
E[b]	21.9	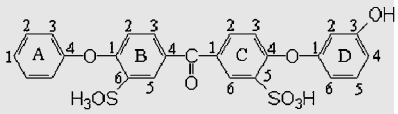
E′[b]	23.6	
E″[b]	and 26.3	

[a] RT, Retention time.
[b] Compound M with an –OH group in *ortho*-, *meta*- and *para*-position.

8.34 (m, 2H, $H_{B5\ and\ C6}$); 6.74 (d, 2 Hz, 1H, H_{D2}); 6.77 (dd, 8.3 Hz–2 Hz, 1H, H_{D4}); 7.37 (t, 8.3 Hz, 1H, H_{D5}); 6.83 (d, 8.3 Hz, 1H, H_{D6}). ^{13}C NMR: Insufficient amount to be analysed. MS (negative mode): *m*/*z* 541 $[M-H]^-$; 270 $[M-2H]^{-2}$.

Table 2
Molar fractions of the different products observed further aging of model compound after complete decomposition of H_2O_2 at *R*2/0.35/80 °C and 130 °C. Data obtained by NMR analysis (precision ± 10–20%).

Products		80 °C	130 °C
M	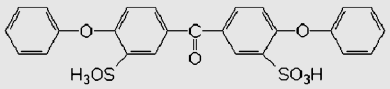	58%[a]	47%[b]
D	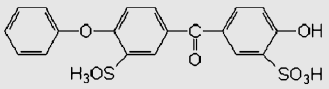	22.5%	24%
B	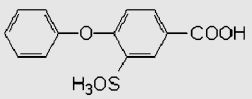	10.5%	10%
C	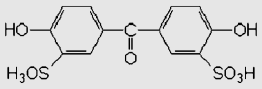	2.5%	3%
	Non identified species	6.5%	16%

[a] 42% are consumed.
[b] 53% are consumed.

3.3. Quantitative analysis

3.3.1. Effect of treatment temperature

A series of experiments were performed to quantify the proportion of each degradation products. For this purpose, three samples containing the same model compound (M) and the same concentration in D_2O were prepared. Hydrogen peroxide was introduced in two samples ($R = 2$) and the same volume of D_2O was added in the last one. After sealing, the tubes containing H_2O_2 were heated respectively at 80 and 130 °C until complete H_2O_2 decomposition. The last sample was considered as a reference whatever the aging temperature as the model molecule thermal stability in water was demonstrated until 130 °C/1500 h. All samples were analysed by NMR. Based on the NMR assignments previously reported (Table 1) to obtain a quantitative measurement one can integrat the signals that do not overlap and that are specific to each structure (M, B, C, D) was determined (Table 2).

It appears clearly that the conversion rate increases with temperature and that degradation leads mainly to the same degradation products (B, C, D) whatever the aging temperature. As their proportion in the final mixture is independent of the treatment temperature, this later parameter should have no significant effect on the aging path involved. However, the proportion of oxidized products included in the unidentified species increases as the temperature treatment is raised (about 6 mol% at 80 °C and 16 mol% at 130 °C). They are characteristic of a high extent of the model molecule degradation.

3.3.2. Effect of treatment duration

Relative proportion evolution of model compound and the main degradation products is reported in Fig. 7 as a function of time at 80 and 130 °C. Different conclusions can be drawn from these experiments.

In both cases, the medium composition varies during the aging process up to a constant final proportion (in good agreement with the values reported on Table 2). As expected, the higher the temperature is, the faster the decomposition is. This observation is consistent with the hydrogen peroxide decomposition kinetics (complete H_2O_2 decomposition after 100 h at 80 °C and after 5 h at 130 °C). H_2O_2 appears as a powerful oxidizing agent because the conversion rate of the model molecule reaches 50% at 130 °C.

The amount of product C remains constant and very low throughout aging. Product B is progressively produced in a low amount. Product D appears in the early steps and accumulates within the degradation process.

3.3.3. Effect of successive degradation steps

The model molecule degradation was investigated for successive hydrogen peroxide additions in order to observe the behaviour of the "primary" degradation products towards further oxidation reactions.

For these experiments, a series of samples were prepared from the same model compound/H_2O_2 solution in D_2O (*R*2/0.58). All samples were aged at 130 °C for 24 h (complete H_2O_2 decomposition) in sealed glass tubes to reduce the time required to perform these aging treatments. Indeed, no chemical difference was observed compared with a thermal treatment realized at 80 °C. While considering one of the samples as a reference for a "first oxidation step", a second H_2O_2 addition and aging treatment at 130 °C were performed for all the other ones. This procedure was repeated five times, leading to five samples corresponding to successive "oxidation steps". The successive addition of aqueous H_2O_2 solution induces a dilution of the samples. Therefore, in order to compare rigorously the different samples, their concentration

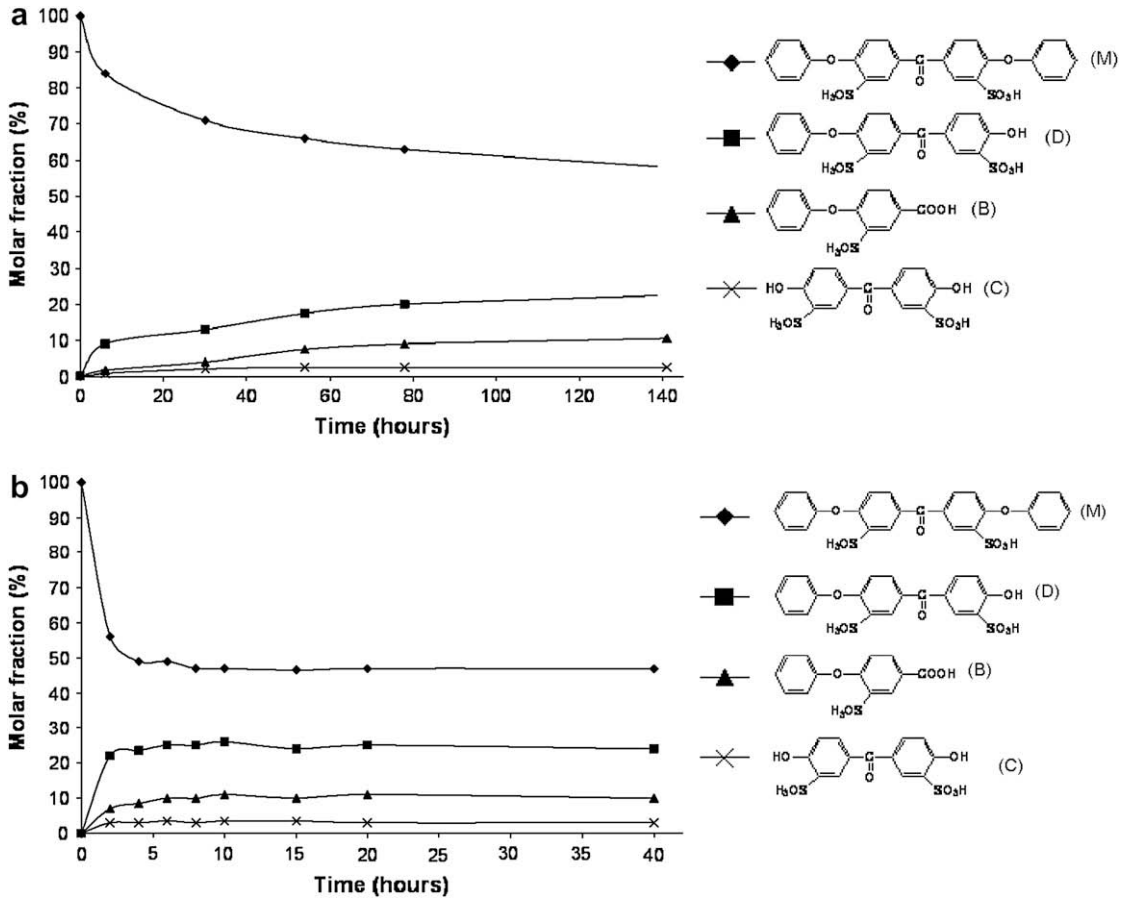

Fig. 7. Evolution of the medium composition during model compound aging experiments: (a) *R*2/0.35/80 °C, (b) *R*2/0.35/130 °C – Data obtained by ^{1}H NMR analysis.

was adjusted with respect to the most diluted one by addition of pure water.

Each sample was analysed by HPLC. Quantification of the different degradation products was carried out by UV detection, monitored at 280 nm. Such a method is attractive since all aromatic degradation products can be studied. Indeed, from an NMR analysis, products A and E could not have been quantified because of overlapping signals.

For the sake of reliability, the evolution of the different products should not be compared to each other as they probably do not have the same molar extinction coefficient. However, significant information can be extracted from the evolution profile of each moiety.

Fig. 8(a) shows the evolution of the amount of each degradation product through five degradation steps. To improve the readability of this graph, curves were normalised to their largest value which has been set to 100 relative units (Fig. 8(b)).

Each H_2O_2 addition degrades around 40% of the model compound (M) present in the sample and five successive oxidation steps are necessary for an almost complete degradation. Product E*, resulting from the addition of a hydroxyl radical OH$^\bullet$ on the model compound reaches its highest concentration during the first degradation step. Further H_2O_2 additions result in a progressive disappearance of this product. This observation can be explained by the well-known low stability of the phenol containing structures in oxidizing media [41,44] and suggests that during successive H_2O_2 additions, the oxidation rate of E* becomes higher than its formation rate. A similar behaviour was observed for D, even if this species seems more stable towards a further oxidation.

While the amounts of E* and D are decreasing over the successive additions of H_2O_2, the quantity of C is increasing. It is obvious that C partly results from a degradation of these compounds.

The amount of product A is all the more important since the degradation process is almost complete. As confirmed by its chemical structure, product A corresponds to high level of oxidation of the initial molecule.

From this study it appears that product E* can be considered as a "primary degradation species" which is further oxidized through successive degradation steps. Product D can be either produced by direct oxidation of model compound (M) or by a further oxidation of E*. In order to determine the main way, the relative proportion of these two products (D and E*) was studied in very mild aging conditions (Table 3). The evolution of the ratio is tabulated for the same amount of model molecule consumed.

These results show that the milder the aging conditions are (the lower H_2O_2 concentration) the higher the proportion of E*/D is. This suggests that product D is produced through the oxidation of E*. However, as the quantity of E* always stays lower than the quantity of D, whatever the investigated aging conditions, a direct oxidation of model M to D cannot be completely excluded. Additional experiments at even lower H_2O_2 concentrations (<0.042%) would have been interesting but in this case the quantification of these degradation products was unfortunately impossible.

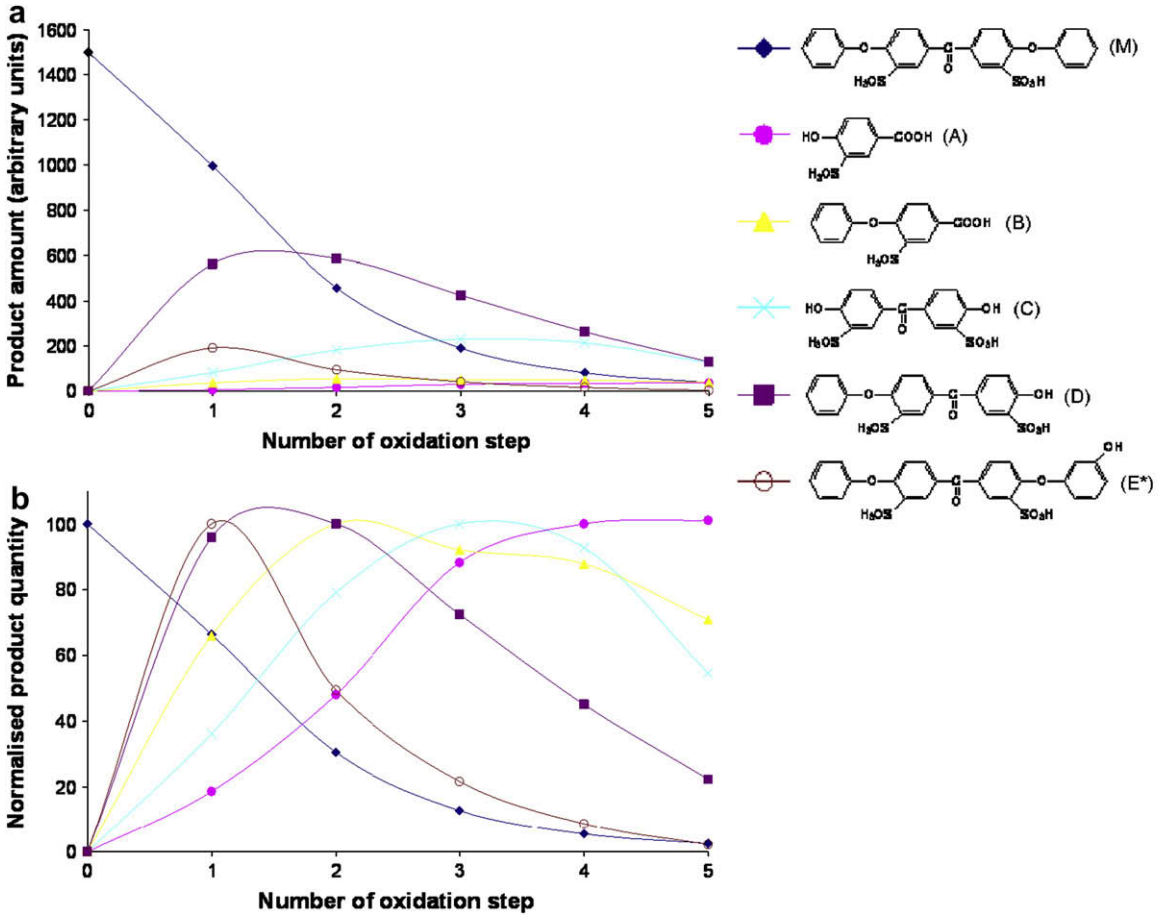

Fig. 8. Amount evolution of each degradation product issued from model compound aging at *R*2/0.58 /130 °C (initially): a) Amount of each product (arbitrary units); b) Normalised quantity of each product (base 100). Data obtained by HPLC analyses ($\lambda = 280$ nm).

4. Model compound decomposition pathway

The oxidative degradation of model compound (M) was shown to induce several bond scissions leading to the formation of different structures containing carboxylic acid (molecule B – Table 1) and hydroxyl or phenol (molecules D and C – Table 1) end groups. One by-product of model compound degradation reaction to D or C should be phenol molecule (induced through the ether cleavage). However, phenol molecule was not detected in our aging conditions. A hypothesis susceptible to explain this phenomenon is related to the high sensitivity of this molecule [41–44] toward oxidation.

In order to confirm this statement, oxidation of phenol was studied in our aging conditions (H_2O_2 0.58 vol%, 130 °C). ^{1}H NMR spectra of the phenol solution before and after aging are presented in Fig. 9. A complete decomposition of phenol was observed after only 1 h aging. HMQC NMR analysis revealed the formation of formic acid, hydroquinone and maleic acid, as mentioned elsewhere by Zazo et al. [44]. After 4 h aging, formic acid is the only compound still present. As shown in Fig. 4, the singlet located between 8.39 and 8.46 ppm (according to the product concentration) corresponds to the formic acid proton. A $J_{H,C}$ coupling constant of 213 Hz was determined between this proton and the carbon of the carboxylic acid group located at 170.6 ppm, the calculated value being of 222 Hz. From these results, formic acid appears as one of the final degradation products of model compound (M). As it was not observed during HPLC separation, it is likely that formic acid has been eliminated during the freeze drying step. Moreover, this compound could not be detected either by mass or UV spectroscopy

Table 3
Relative proportions of product E* and D formed during the model compound aging treatment at 80 °C – Data obtained by HPLC analysis.

$R = (H_2O_2/\text{Model})$ (mole)	H_2O_2 initial concentration (vol%)	E* over D ratio
0.25	0.045	0.73
0.5	0.09	0.15
1	0.17	0.05
2	0.58	0.03 at 130 °C

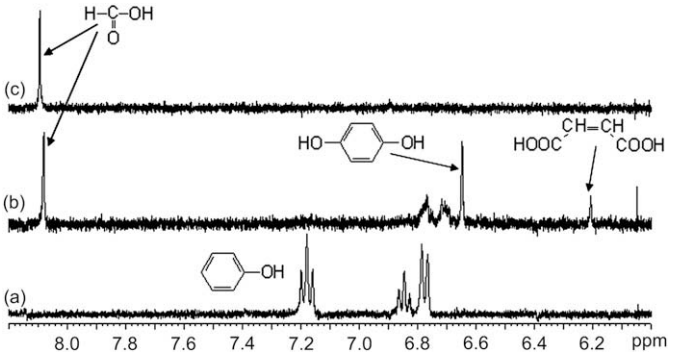

Fig. 9. ^{1}H NMR spectra of phenol in a H_2O_2 0.58 vol% solution: a) un-aged phenol; b) after 1 h at 130 °C; c) after 4 h at 130 °C.

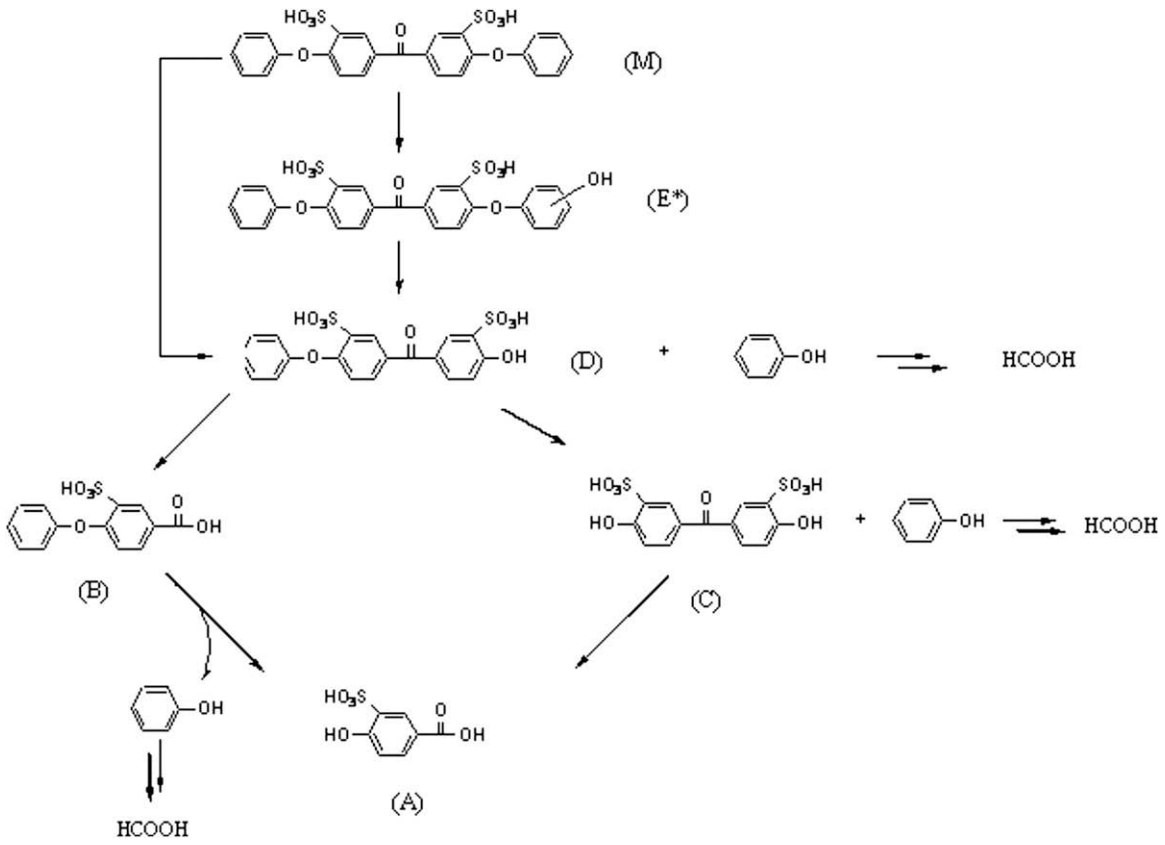

Scheme 1. Model compound degradation mechanism in the presence of hydrogen peroxide.

as it does not absorb significantly in the studied UV region and as its molecular weight is below the detection limit of the MS apparatus.

All the results obtained in this study suggest that the first step of model compound (M) oxidation is the addition of a hydroxyl radical on the non-sulfonated phenyl ether aromatic ring. This is in good agreement with the work of Hübner and Roduner [37], as the presence of electron-withdrawing groups is reported to disfavour the addition of HO•. As witnessed by the LC–MS analysis (Fig. 4), three isomers of product E*, bearing a hydroxyl group in *ortho*-, *meta*- and *para*-positions of the phenyl ether bridge, were detected. Whereas the *meta*-isomer was present in a sufficient amount to be fully characterised by NMR, the other isomers were produced in very low quantities. This experimental observation is in good agreement with the predictive modelisation work of Panchenko [54].

A simultaneous addition of a hydroxyl radical HO• on each phenyl ether ring was not evidenced. However, as the chemical stability of the degradation products E* appears limited in these aging conditions, their concentration remaining very low through aging, this degradation product should have a very limited life time.

Through successive oxidations steps, these phenol species do not accumulate in the medium. They progressively disappear on behalf of the appearance of other degradation products. This is not surprising with regard to the high sensitivity of such structures towards oxidizing agents [41–44]. As reported by Hübner and Roduner [23], the presence of a hydroxyl group even favours further oxidation reactions. This is corroborated by the appearance of product D in the reaction medium. In turn, this species, which is very sensitive to oxidizing conditions, leads to the formation of products B and C. Finally, product A corresponds to a high oxidation level of the model compound (M).

From these considerations, a general degradation path of model compound (M) in the oxidative experimental conditions has been established (Scheme 1).

A direct scission of ether bonds (without any former hydroxyl radical addition) cannot be excluded but such a mechanism is not consistent with two observations. First, the amount of product C remains very low whereas the amount of product B goes up (Fig. 7(a)). Moreover, the probability to have simultaneously two ether scissions must be very low and the induced product is very sensitive to oxidation. As a consequence, the degradation kinetics of C should be faster than B and the highest concentration of C should be obtained at the first step of degradation (Fig. 8(b)). However we can observe that the highest concentration of C is reached after three peroxide additions. Therefore, this mechanism is considered as minor in the proposed route for the model compound oxidation.

On the basis of this aging mechanism, the sensitivity of the aromatic ring to hydroxyl radical attack must be reduced to improve sulfonated polyaromatic membrane durability. One way should be to replace the ether linkage by a withdrawing group like a sulfoxide one. Another way should be to avoid addition reaction in the *meta* position with pendant group attached on the aromatic ring.

5. Conclusion

A model compound mimicking the hydrophilic sequence of a sulfonated poly(aryl ether ketone) was synthesized by aromatic nucleophilic substitution. This compound was aged from 60 to 130 °C, in the presence of hydrogen peroxide. Seven "aged products" were detected by analytical HPLC analysis. However two of them were in a too low concentration to be collected in a sufficient

amount to perform extensive analyses on them. Consequently, thanks to a preparative HPLC fractionation, only five main species were collected. The elucidation of their chemical structures was performed by a thorough characterization, thanks to different analytical techniques (^{1}H and ^{13}C NMR, IR and Mass Spectroscopy). In a series of experiments corresponding to successive oxidation steps, the evolution of the relative quantities of each product was studied. From the results obtained, a degradation mechanism of the sulfonated aryl ether ketone model and a strategy to improve the stability of this sequence were proposed.

In order to check the validity of such a mechanism on a macromolecular compound and to verify if the same aged species are produced during a fuel cell test, analogous experiments are currently under progress on high molecular weight sulfonated poly(arylether ketone)s. To conclude, our results demonstrate that a model compound stability study is a powerful strategy to identify the best stable chemical structures which could be used as membrane in fuel cell.

Acknowledgment

This work has been performed in the framework GDR 2985 PACTE for financial support and Jean Jacques Allegraud for chromatographic technical support.

References

[1] Yu J, Yi B, Xing D, Liu F, Shao Z, Fu Y, et al. Degradation mechanism of polystyrene sulfonic acid membrane and application of its composite membranes in fuel cells. Physical Chemistry Chemical Physics 2003;5:611.
[2] Daletou MK, Gourdoupi N, Kallitsis JK. Proton conducting membranes based on blends of PBI with aromatic polyethers containing pyridine units. Journal of Membrane Science 2005;252:115.
[3] Holladay JD, Wainright JS, Jones EO, Gano SR. Power generation using a mesoscale fuel cell integrated with a microscale fuel processor. Journal of Power Sources 2004;130:111.
[4] Pu H, Liu Q, Liu G. Methanol permeation and proton conductivity of acid-doped poly(N-ethylbenzimidazole) and poly(N-methylbenzimidazole). Journal of Membrane Science 2004;241:169.
[5] Qing S, Huang W, Yan D. Synthesis and characterization of thermally stable sulfonated polybenzimidazoles. European Polymer Journal 2005;41(7):1589–95.
[6] Jouanneau J, Mercier R, Gonon L, Gebel G. Synthesis of sulfonated polybenzimidazoles from functionalized monomers: preparation of ionic conducting membranes. Macromolecules 2007;40:983.
[7] Genies C, Mercier R, Sillion B, Cornet N, Gebel G. Soluble sulfonated naphthalenic polyimides as materials for proton exchange membranes. Polymer 2001;42:359.
[8] Geniès C, Mercier R, Sillion B, Petiaud R, Cornet N, Gebel G, et al. Stability study of sulfonated phthalic and naphthalenic polyimide structures in aqueous medium. Polymer 2001;42:5097.
[9] Gunday ST, Bozkurt A, Aghatabay NM, Baykal AH. Benzimidazole tethered proton conducting organic electrolytes, Materials Chemistry and Physics, in press, corrected proof.
[10] Meyer G, Gebel G, Gonon L, Capron P, Marscaq D, Marestin C, et al. Degradation of sulfonated polyimide membranes in fuel cell conditions. Journal of Power Sources 2006;157:293.
[11] Meyer G, Perrot C, Gebel G, Gonon L, Morlat S, Gardette J-L. Ex situ hydrolytic degradation of sulfonated polyimide membranes for fuel cells. Polymer 2006;47:5003.
[12] Guo X, Fang J, Watari T, Tanaka K, Kita H, Okamoto K-i. Novel sulfonated polyimides as polyelectrolytes for fuel cell application. 2-Synthesis and proton conductivity of polyimides from 9,9-bis(4-aminophenyl)fluorene-2,7-disulfonic acid. Macromolecules 2002;35:6707.
[13] Einsla BR, Kim YS, Hickner MA, Hong Y-T, Hill ML, Pivovar BS, et al. Sulfonated naphthalene dianhydride based polyimide copolymers for proton-exchange-membrane fuel cells II. Membrane properties and fuel cell performance. Journal of Membrane Science 2005;255:141.
[14] Kim H-j, Litt MH, Nam SY, Shin E-m. Synthesis and characterization of sulfonated polyimide polymer electrolyte membranes. Macromolecular Research 2003;11:458.
[15] Lee C, Sundar S, Kwon J, Han H. Structure-property correlations of sulfonated polyimides. II-Effect of substituent groups on membrane properties. Journal of Polymer Science: Part A: Polymer Chemistry 2004;42:3621.
[16] Asano N, Suzuki S, Miyatake K, Uchida H, Watanabe M. Aliphatic/aromatic polyimide ionomers as a proton conductive membrane for fuel cell applications. Journal of American Chemical Society 2006;128:1762.
[17] Harrison WL, Hickner MA, Kim YS, McGrath JE. Poly(arylene ether sulfone) copolymers and related systems from disulfonated monomer building blocks: synthesis, characterization, and performance – a topical review. Fuel Cells 2005;5:201.
[18] Taeger A, Vogel C, Lehmann D, Lenk W, Schlenstedt K, Meier-Haack J. Sulfonated multiblock copoly(ether sulfone)s as membrane materials for fuel cell applications. Macromolecular Symposia 2004;210:175.
[19] Wang Z, Li X, Zhao C, Ni H, Na H. Synthesis and characterization of sulfonated poly(arylene ether ketone ketone sulfone) membranes for application in proton exchange membrane fuel cells, Journal of Power Sources Special issue including selected papers presented at the International Workshop on Molten Carbonate Fuel Cells and Related Science and Technology 2005 together with regular papers, 160 (2006) 969.
[20] Aoki M, Chikashige Y, Miyatake K, Uchida H, Watanabe M. Durability of novel sulfonated poly(arylene ether) membrane in PEFC operation. Electrochemistry Communications 2006;8:1412.
[21] Xing P, Robertson GP, Guiver MD, Mikhailenko SD, Kaliaguine S. Sulfonated poly(aryl ether ketone)s containing the hexafluoroisopropylidene diphenyl moiety prepared by direct copolymerization, as proton exchange membranes for fuel cell application. Macromolecules 2004;37:7960.
[22] Xing P, Robertson GP, Guiver MD, Mikhailenko SD, Kaliaguine S. Synthesis and characterization of poly(aryletherketone) copolymers containing (hexafluoroisopropylidene)-diphenol moiety as proton exchange membrane materials. Polymer 2005;46:3257.
[23] Hübner G, Roduner E. EPR investigation of HO•radical initiated degradation reactions of sulfonated aromatics as model compounds for fuel cell proton conducting membranes. Journal of Materials Chemistry 1999;9:409.
[24] Alberti G, Casciola M, Massinelli L, Bauer B. Polymeric proton conducting membranes for medium temperature fuel cells (110–160 °C). Journal of Membrane Science 2001;185:73.
[25] Bauer B, Jones DJ, Rozière J, Tchicaya L, Alberti G, Casciola M, et al. Electrochemical characterisation of sulfonated polyetherketone membranes. Journal of New Materials for Electrochemical Systems 2000;3:93.
[26] Rozière J, Jones DJ. Non-fluorinated polymer materials for proton exchange membrane fuel cells. Annual Review of Materials Research 2003;33:503.
[27] Zhao C, Li X, Wang Z, Dou Z, Zhong S, Na H. Synthesis of the block sulfonated poly(ether ether ketone)s (S-PEEKs) materials for proton exchange membrane. Journal of Membrane Science 2006;280:643.
[28] Miyatake K, Oyaizu K, Tsuchida E, Hay AS. Synthesis and properties of novel sulfonated arylene ether/fluorinated alkane copolymers. Macromolecules 2001;34:2065.
[29] LaConti AB, Mamdan M, McDonald RC. In: Vielstich W, Gasteiger HA, Lamm A, editors. Handbook of fuel cells, vol. 3. New York: John Wiley & Sons; 2003.
[30] Antoine O, Durand R. RRDE study of oxygen reduction on Pt nanoparticles inside Nafion®: H_2O_2 production in PEMFC cathode conditions. Journal of Applied Electrochemistry 2000;30:839.
[31] Collier A, Wang H, Zi Yuan X, Zhang J, Wilkinson DP. Degradation of polymer electrolyte membranes. International Journal of Hydrogen Energy Fuel Cells 2006;31:1838.
[32] Inaba M, Yamada H, Tokunaga J, Tasaka A. Effect of agglomeration of Pt/C catalyst on hydrogen peroxide formation. Electrochemical and Solid State Letters 2004;7:A474.
[33] Inaba M, Kinumoto T, Kiriake M, Umebayashi R, Tasaka A, Ogumi Z. Gas crossover and membrane degradation in polymer electrolyte fuel cells. Electrochimica Acta 2006;51:5746.
[34] Kadirov MK, Bosnjakovic A, Schlick S. Membrane-derived fluorinated radicals detected by electron spin resonance in UV-irradiated Nafion and Dow ionomers: effect of counterions and H_2O_2. Journal of Physical Chemistry B 2005;109:7664.
[35] Kinumoto T, Inaba M, Nakayama Y, Ogata K, Umebayashi R, Tasaka A, Iriyama Y, Abe T, Ogumi Z. Durability of perfluorinated ionomer membrane against hydrogen peroxide, Journal of Power Sources Special issue including selected papers from the 6th International Conference on Lead-Acid Batteries (LABAT 2005, Varna, Bulgaria) and the 11th Asian Battery Conference (11 ABC, Ho Chi Minh City, Vietnam) together with regular papers, 158 (2006) 1222.
[36] Liu W, Zuckerbrod D. In situ detection of hydrogen peroxide in PEM fuel cells. Journal of the Electrochemical Society 2005;152:A1165.
[37] Mitov S, Delmer O, Kerres J, Roduner E. Oxidative and photochemical stability of ionomers for fuel-cell membranes. Helvetica Chimica Acta 2006;89:2354.
[38] Panchenko A, Dilger H, Kerres J, Hein M, Ullrich A, Kaz T, et al. In-situ spin trap electron paramagnetic resonance study of fuel cell processes. Physical Chemistry Chemical Physics 2004;6:2891.
[39] Schmidt TJ, Paulus UA, Gasteiger HA, Behm RJ. The oxygen reduction reaction on a Pt/carbon fuel cell catalyst in the presence of chloride anions. Journal of Electroanalytical Chemistry 2001;508:41.
[40] Tang H, Peikang S, Jiang SP, Wang F, Pan M. A degradation study of Nafion proton exchange membrane of PEM fuel cells. Journal of Power Sources 2007;170:85.
[41] Alnaizy R, Akgerman A. Advanced oxidation of phenolic compounds. Advances in Environmental Research 2000;4:233.

[42] Devlin HR, Harris IJ. Mechanism of the oxidation of aqueous phenol with dissolved oxygen. Industrial & Engineering Chemistry Fundamentals 1984;23:387.
[43] Santos A, Yustos P, Quintanilla A, Rodriguez S, Garcia-Ochoa F. Route of the catalytic oxidation of phenol in aqueous phase. Applied Catalysis B: Environmental 2002;39:97.
[44] Zazo JA, Casas JA, Mohedano AF, Gilarranz MA, Rodriguez JJ. Chemical pathway and kinetics of phenol oxidation by Fenton's reagent. Environmental Science and Technology 2005;39:9295.
[45] Liu B, Kim D-S, Murphy J, Robertson GP, Guiver MD, Mikhailenko S, et al. Fluorenyl-containing sulfonated poly(aryl ether ether ketone ketone)s (SPFEEKK) for fuel cell applications. Journal of Membrane Science 2006;280:54.
[46] Yin Y, Fang J, Cui Y, Tanaka K, Kita H, Okamoto K-i. Synthesis, proton conductivity and methanol permeability of a novel sulfonated polyimide from 3-(2′,4′-diaminophenoxy)propane sulfonic acid. Polymer 2003;44:4509.
[47] Marechal M, Wessel R, Diard J-P, Guindet J, Sanchez J-Y. Study of PEMFC ionomers through model molecules mimicking the ionomer repeat units. Electrochimica Acta 2007;52:7953.
[48] Wang F, Chen TL, Xu JP. Sodium sulfonate-functionalized poly(ether ether ketone)s. Macromolecular Chemistry and Physics 1998;199:1421.
[49] Meier-Haack J, Taeger A, Vogel C, Schlenstedt K, Lenk W, Lehmann D. Membranes from sulfonated block copolymers for use in fuel cells. Separation and Purification Technology 2005;41:207.
[50] Iojoiu C, Genova-Dimitrova P, Marechal M, Sanchez J-Y. Chemical and physicochemical characterizations of ionomers. Electrochimica Acta 2006;51:4789.
[51] Wu H-L, Ma C-CM, Liu F-Y, Chen C-Y, Lee S-J, Chiang C-L. Preparation and characterization of poly(ether sulfone)/sulfonated poly(ether ether ketone) blend membranes. European Polymer Journal 2006;42:1688.
[52] Breitmaier EV, Wolfgang. Carbon-13 NMR spectroscopy. 3rd ed. New York: John Wiley and Sons Ltd; 1987.
[53] Ewing DF. C-13 substituent effects in monosubstituted benzenes. Organic Magnetic Resonance 1979;12:499.
[54] Panchenko A. DFT investigation of the polymer electrolyte membrane degradation caused by OH radicals in fuel cells. Journal of Membrane Science 2006;278:269.